

Multifractal clustering of passive tracers on a surface flow

G. BOFFETTA¹, J. DAVOUDI², F. DE LILLO³

¹ *Dipartimento di Fisica Generale and INFN, Università degli Studi di Torino, Via Pietro Giuria 1, 10125, Torino, Italy*

and ISAC-CNR, Sezione di Torino, Italy

² *Fachbereich Physik, Philipps-Universität, Renthof 6, D-35032 Marburg, Germany*

³ *INLN-CNRS, 1361 route des Lucioles, Sophia Antipolis, 06560 Valbonne, France.*

PACS. 47.27.Gs – Isotropic turbulence; homogeneous turbulence.

PACS. 47.52.+j – Chaos.

Abstract. –

We study the anomalous scaling of the mass density measure of Lagrangian tracers in a compressible flow realized on the free surface on top of a three dimensional flow. The full two dimensional probability distribution of local stretching rates is measured. The intermittency exponents which quantify the fluctuations of the mass measure of tracers at small scales are calculated from the large deviation form of stretching rate fluctuations. The results indicate the existence of a critical exponent $n_c \simeq 0.86$ above which exponents saturate, in agreement with what has been predicted by an analytically solvable model. Direct evaluation of the multifractal dimensions by reconstructing the coarse-grained particle density supports the results for low order moments.

Advection of homogeneous distribution of passive particles in a compressible flow generically results in clusters of particles' concentration [1–3]. The effects of compressibility in three-dimensional flows are typically relevant only at Mach numbers near or larger than 1 when density inhomogeneity reacts back on the fluid velocity. However there are simple physical systems in which the phenomenology of passive particle advection in compressible flows is applicable. Effective flows of inertial particles in incompressible flows at small Stokes numbers [4–6] and flows of surface suspensions [7–9] are among such instances.

Consider the distribution of particles advected by a velocity field $\mathbf{u}(\mathbf{x}, t)$ assumed homogeneous and stationary in time. The evolution of particle density $\rho(\mathbf{x}, t)$ in the limit of vanishing diffusivity is given by

$$\frac{\partial \rho}{\partial t} + \nabla \cdot (\rho \mathbf{u}) = 0 \quad (1)$$

If $\nabla \cdot \mathbf{u} \neq 0$ the flow is compressible and particle trajectories asymptotically converge to a non-uniform distribution. Compressibility can be characterized by the dimensionless ratio $\mathcal{C} = \frac{\langle (\partial_i u_i)^2 \rangle}{\langle (\partial_i u_j)^2 \rangle}$ which assumes values in $0 \leq \mathcal{C} \leq 1$, the limiting values corresponding to an incompressible and a potential flow respectively. The particle density depends on the particular realization of the velocity field and for a stationary random flow the density is expected to converge to a statistically stationary state ρ_* .

A suitable way to characterize the statistics of the density field on the attractor is to measure the *Lagrangian* moments of the coarse-grained mass in a small region of size r as:

$$\langle m_r^n \rangle = \overline{\int \rho_*(\mathbf{x}) m_r^n(\mathbf{x}) d\mathbf{x}} \quad (2)$$

where $m_r(\mathbf{x}) = \int_{B_r(\mathbf{x})} \rho_*(\mathbf{x}') d\mathbf{x}'$ is the coarse-grained mass in a ball of radius r centered at \mathbf{x} . The weight ρ_* in (2) restricts the average to balls centered on the attractor. Note that the coarse grained mass $m_r(\mathbf{x})$ depends on the specific velocity configuration within a given ensemble of flow realizations: the $\overline{(\dots)}$ means the averaging with respect to the given velocity statistics.

When $r \rightarrow 0$ and under generic assumptions for the random flow $\langle m_r^n \rangle \sim r^{\xi_n}$ [3,10]. A non-linear dependence of the set of scaling exponents ξ_n on the order n implies an *intermittent* distribution of mass fluctuations at small scales. Recently, a phenomenological connection between the probability distribution of small scale velocity stretching rates and scaling exponents of coarse grained mass moments has been obtained [11]. More precisely the set of exponents ξ_n are bridged to the Cramer function of the stretching rates of the underlying flow. It is shown that ξ_n saturates at large n . The saturation is a footprint of the very violent events which spoil the scaling in the higher mass moments.

Here we study the clustering of passive tracers which move on the two-dimensional free slip surface on the top of a three-dimensional incompressible fluid [8,9]. Our main result is that an intermittent distribution of passive tracers, with saturation of high-order scaling exponents, is observed also in this realistic, time correlated flow.

When the flow is spatially smooth the evolution of trajectories is a combination of random stretching and contracting in time. The individual tracers are advected by the same realization of the flow thus the evolution of the separation between two Lagrangian particles is given by $\mathbf{X}(t, \mathbf{x}) = \mathbf{W}(t, \mathbf{x})\mathbf{X}(0, \mathbf{x})$ where $\mathbf{X}(0, \mathbf{x})$ is the initial separation. The linear random stretching and contracting is encoded in the positive eigenvalues of the symmetric matrix $W^\dagger(t, x)W(t, x)$: $e^{2t\sigma_1}, \dots, e^{2t\sigma_d}$. The *forward stretching rates* $\sigma_i(t)$ are arranged in non-decreasing order and asymptotically converge to the *Lyapunov* exponents at large times, i.e. $\lambda_i = \lim_{t \rightarrow \infty} \sigma_i$ [3]. For generic cases when the spectrum is non-degenerate the local stretching rates satisfy an asymptotic probability distribution function (PDF) with the following large deviation shape [12],

$$P(\sigma_1, \dots, \sigma_d; t) \sim e^{-tH(\sigma_1, \dots, \sigma_d)}, \quad (3)$$

where the Cramer function $H(\sigma_1, \dots, \sigma_d) \geq 0$ is convex and takes its minimum in $H(\lambda_i) = 0$.

For completeness, here we briefly sketch the outline of the theoretical arguments first appeared in [11]. In a two-dimensional compressible flow, the Lagrangian evolution correspond to a dissipative dynamics with $\sigma_1 > 0$ and $\sigma_2 < 0$ and with $\sum_i \sigma_i \leq 0$. Along the unstable direction the density is smooth while in the stable direction the density configuration is fractal. After a transient regime the density is expected to reach to statistical stationary state. We will take formally the initial time $t_0 \rightarrow -\infty$ thus we will assume that at $t = 0$ the density ρ_* is already stationary. At time $t > 0$ one looks at the fluctuation of the coarse-grained mass generated by ρ_* according to (2). Consider a rectangular box of size r with sides r_1 and r_2 along the orthogonal unstable and stable directions. According to eq.(2) $\langle m_{r_1, r_2}^n \rangle \sim r_1^{\xi_n^{(1)}} r_2^{\xi_n^{(2)}}$ where $\xi_n = \xi_n^{(1)} + \xi_n^{(2)}$. Since the measure along the unstable direction r_1 is regular one gets $\xi_n^{(1)} = \min(\xi_n, n)$. For $\xi_n \geq n$ it results to $\xi_n^{(1)} = n$ and therefore $\langle m_{r_1, r_2}^n \rangle \sim r_1^n r_2^{\xi_n - n}$. In the case of $\xi_n < n$ it reads $\langle m_{r_1, r_2}^n \rangle \sim r_1^{\xi_n} r_2^0$.

The pre-image of the box at time $t = 0$ is a stretched box as r_1 shrinks to $r_1 e^{-t\sigma_1}$ and r_2 increases to $r_2 e^{-t\sigma_2}$. Due to conservation of the mass and stationarity the mass moments in the pre-image box at time $t = 0$ are the same, i.e.

$$\langle m_{r_1, r_2}^n \rangle \sim \langle m_{r_1 e^{-t\sigma_1}, r_2 e^{-t\sigma_2}}^n \rangle. \quad (4)$$

According to the definition in (2) the average on the right hand side is considered over the distribution of the forward stretching rate with respect to invariant measure ρ_* . Note that the result of averaging over forward and backward distributions with respect to invariant measure are the same [13]. At large time t one resorts on the saddle point argument whereby two distinct situations emerges from eq.(4) that is,

$$\min_{\sigma_1, \sigma_2} \{H(\sigma_1, \sigma_2) + n\sigma_1 + (\xi_n - n)\sigma_2\} = 0 \quad n \leq \xi_n, \quad (5)$$

$$\min_{\sigma_1, \sigma_2} \{H(\sigma_1, \sigma_2) + \xi_n \sigma_1\} = 0 \quad n \geq \xi_n. \quad (6)$$

The above relations connect the scaling exponents ξ_n to the Cramer function $H(\sigma_1, \sigma_2)$. For a synthetic Gaussian and white in time smooth flows (the Kraichnan model of turbulence [14]) where the exact functional form of Cramer function is known, eqs. (5-6) lead to an analytic form for the scaling exponents [11]:

$$\xi_n = \begin{cases} \frac{2n + \sqrt{(1+2\mathcal{C})^2 - 8\mathcal{C}n^2}}{1+2\mathcal{C}} - 1 & \text{if } n \leq n_c, \\ \xi_\infty & \text{if } n \geq n_c \end{cases} \quad (7)$$

where the critical order for saturation is given by

$$n_c = \begin{cases} \frac{1}{2} \sqrt{1 + \frac{1}{2\mathcal{C}}} & \text{if } 0 < \mathcal{C} \leq \frac{1}{6}, \\ \frac{2-4\mathcal{C}}{1+2\mathcal{C}} & \text{if } \frac{1}{6} \leq \mathcal{C} < \frac{1}{2}. \end{cases} \quad (8)$$

In the general case, depending on the flow compressibility \mathcal{C} two scenarios for saturation are thus conceivable. In the first scenario the line $\xi_n = \xi_\infty$ from (6) intersects with the curve of $\xi_n(n)$ given by (5). In such a case $\xi_\infty = \xi_{n_c} = n_c$ and the value of $(\sigma_1^*(n_c), \sigma_2^*(n_c))$ will pass through the line $\sigma_1 = \sigma_2$. In the second case the line tangent to the maximum of the manifold $\xi_n(n)$ given by (5) identifies ξ_∞ . In this later scenario $\xi_{n_c} \neq n_c$ and n_c identifies with the solution of $\frac{d\xi_n}{dn}|_{n_c} = 0$. For the Kraichnan model the second case results in $\xi_\infty = \xi_{n_c} = 2n_c - 1$.

We have integrated the three-dimensional Navier-Stokes equation for an incompressible flow by means of a standard pseudo-spectral code at resolution 64^3 . Lateral boundary conditions for x and y directions are periodic, while in the vertical z direction we apply free-slip boundary conditions, $u_z = 0$ and $\partial_z u_x = \partial_z u_y = 0$ [7]. When the flow is in statistically stationary conditions, 10^5 passive tracers are placed on the top free surface $z = 0$. Their two dimensional positions $\mathbf{x}(t) = (x(t), y(t))$ are advected by the two-dimensional flow (u_x, u_y) which is compressible since $\partial_x u_x + \partial_y u_y = -\partial_z u_z \neq 0$ [8, 9]. The compressibility of the surface flow was found to be $\mathcal{C} \simeq 0.21$.

In order to evaluate the stretching rates, we have integrated along each trajectory a set of two orthogonal tangent vectors $\mathbf{z}^{(k)}$ ($k = 1, 2$) evolving according to

$$\frac{d}{dt} z_i^{(k)} = (\nabla_j u_i) z_j^{(k)} \quad (i, j = 1, 2) \quad (9)$$

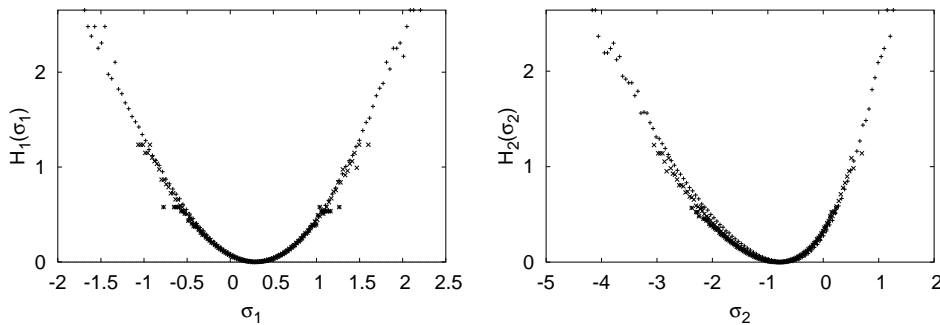


Fig. 1 – Marginal Cramer functions $H_1(\sigma_1)$ (left) and $H_2(\sigma_2)$ (right) computed at three different times lags $\tau = \lambda_1^{-1}$, $\tau = 2\lambda_1^{-1}$ and $\tau = 4\lambda_1^{-1}$.

The PDF of stretching rates at fixed time lag τ , $P(\sigma_1, \sigma_2; \tau)$, is then accumulated by computing $\sigma_k = (1/\tau) \ln(|z^{(k)}(\tau)|/|z^{(k)}(0)|)$ for different realizations along the trajectories.

Stretching rate statistics are accumulated up to $t_{max} = 15000\lambda_1^{-1}$ which correspond to about 7000 velocity correlation times $T \simeq 2.1\lambda_1^{-1}$. The fluctuations of each of the stretching rates is quantified by the convergence of their corresponding marginal Cramer functions $H_i(\sigma_i)$. These are defined as

$$P_i(\sigma_i; t) = \int P(\sigma_1, \sigma_2; t) d\sigma_{3-i} \sim e^{-tH_i(\sigma_i)} ; i = 1, 2, \quad (10)$$

Fig.1 shows the two marginal Cramer functions obtained from the marginal probability density functions of stretching rates at three different time lags $\tau = \lambda_1^{-1}$, $\tau = 2\lambda_1^{-1}$ and $\tau = 4\lambda_1^{-1}$. The average values of stretching rates, i.e. the minimum of the marginal Cramer functions, converge to the Lyapunov exponents $\lambda_1 \simeq 0.29$, $\lambda_2 \simeq -0.86$ from which one estimates the Lyapunov dimension [3] as $D_L = 1 + \frac{\lambda_1}{|\lambda_2|} \simeq 1.34$. This value is larger to what obtained in a similar set of simulations at higher Reynolds numbers [9], but is consistent with the fact that here the value of compressibility is smaller.

In Fig.(2) we present the contour plot of the two dimensional Cramer function $H(\sigma_1, \sigma_2)$ evaluated at three different time lags. The overlap of the contour corresponding to different time delays is the indication of the convergence of the statistics. We observe that the contours are rather far from an elliptic shape, a direct indication of the deviations of the probability density $P(\sigma_1, \sigma_2; \tau)$ from a Gaussian distribution (as it is also evident from the marginal distributions in Fig. 1).

From the Cramer function $H(\sigma_1, \sigma_2)$ the set of scaling exponents ξ_n is obtained by numerical minimization of relations (5)-(6). For each order n this procedure determines a point $(\sigma_1^*(n), \sigma_2^*(n))$ in the stretching rate plane. The line in Fig.(2) represents the trajectory of these points starting from $n = 0$ to $n = n_c \simeq 0.86$ where the point crosses the line $\sigma_1 = \sigma_2$ and the exponents saturates, for $n \geq n_c$, to $\xi_n = n_c$, following the second of the two scenarios described above.

The set of scaling exponents obtained from the minimization of Cramer function is shown in Fig. 3. Intermittency of mass distribution is evident from the non-linear behavior of ξ_n .

The geometrical interpretation of the saturation predicted by (6) is that the intersection between the line $-\xi_{n_c}\sigma_1$ and the curve $H(\sigma_1, \sigma_2^*(n_c))$ is tangent at $n = n_c$. In the inset of Fig. 3 we show that this is indeed reproduced by our data and that the tangent point is well

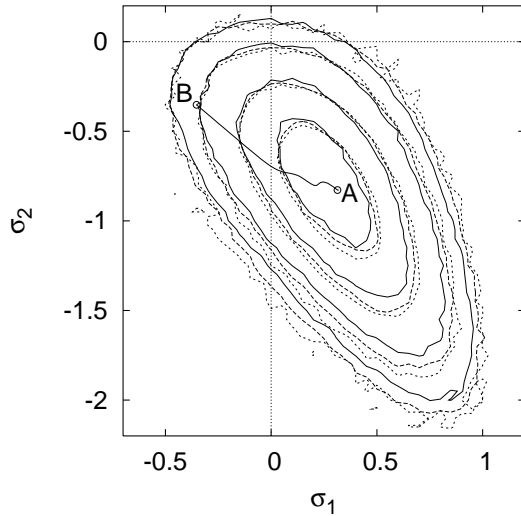


Fig. 2 – Two dimensional contour plots of the Cramer functions $H(\sigma_1, \sigma_2)$ computed at three different times $\tau = \lambda^{-1}$, $\tau = 2\lambda^{-1}$ and $\tau = 4\lambda^{-1}$. The geometrical locus of $(\sigma_1^*(n), \sigma_2^*(n))$ is shown from $n = 0$ (A) to $n = n_c \simeq 0.86$ (B).

inside the convergence range. This result indicates that the saturation observed in Fig. 3 is a genuine phenomenon and it is not induced by finite size statistics.

We have compared the scaling exponents determined by the stretching rates with those directly measured from the mass distribution. To this aim, we stored 12000 configurations of the 10^5 particles at an interval $\Delta t = 0.67T$. Particle density $\rho(\mathbf{x})$ is reconstructed by distributing the positions of the Lagrangian tracers on a regular grid of resolution 512×512 . For each snapshot we directly measure the coarse-grained mass and calculate the mass moments $\langle m_r^n \rangle$ according to Eq.(2). The moments are then averaged over the 12000 snapshots and the scaling exponents are estimated by a best fit. The box-counting scaling exponents $\xi_n^{(BC)}$ are shown in Fig. 3 up to order $n = 1.3$.

As it is evident from the figure the moments are extremely fluctuating. The low order exponents, for $n \leq n_c$, are very close to the values obtained from minimization of Cramer function. The saturation of the scaling exponents is corresponding to the rare events when large fraction of the particles accumulate at very small scales. For $n > n_c$ the box counting exponents deviate from the saturation line, but we have found that the distribution strongly fluctuates from one realization to another.

In order to estimate the magnitude of these fluctuations, we have computed, for each realization, the maximum fraction of particles in a single grid cell, i.e. n_{\max}/N . The resulting distribution is shown in Fig 4 which shows a rather fat tail with events up to $n_{\max}/N \simeq 0.4$. This value of concentration has to be compared with the most probable value $n_{\max}/N \simeq 0.009$ (see Fig 4).

These configurations of extreme concentration are responsible for the saturation of scaling exponents. Indeed, if we compute the box-counting exponents $\xi_n^{(BC)}$ for one of these particular configuration, we observe a saturation of the exponents at a value even smaller than ξ_∞ (see Fig. 3). Although our data provides sufficient statistics to measure the joint distribution of local stretching rates the dynamical evolution of the rare events responsible for saturation of

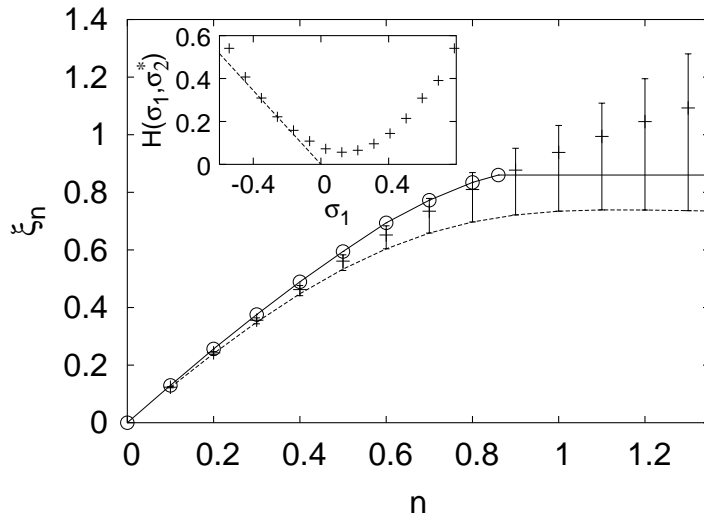


Fig. 3 – Scaling exponents ξ_n computed from the stretching-rate analysis (connected circles). The horizontal line for $n > n_c \simeq 0.86$ represents the saturation value $\xi_\infty = n_c$. Scaling exponents obtained from a direct box-counting analysis are shown after averaging 60 sets of 200 configurations each (+, error bars estimated on the fluctuations among different sets). The lower line is the result of the direct computation of mass exponents for the particular subset where saturation is observed (see Fig. 4).

the coarse grained mass requires by far a longer sampling. This explains the large level of fluctuation for $\xi_n^{(BC)} \geq n$ in Fig. 3.

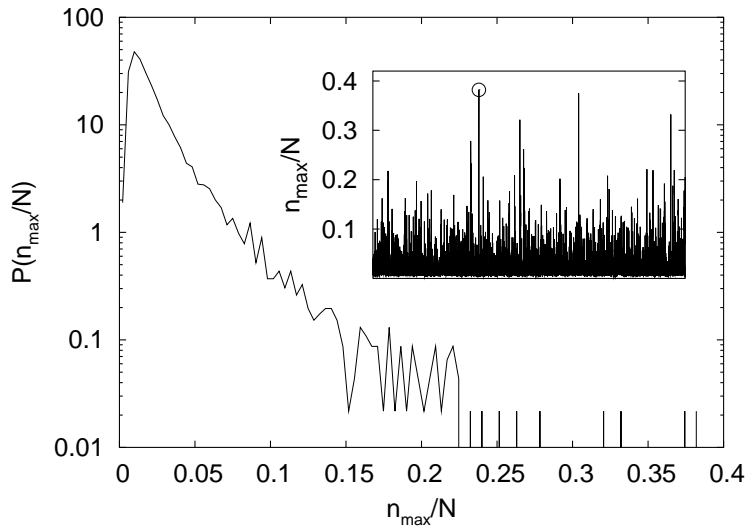


Fig. 4 – The distribution of the maximum fraction of particles contained in a single bin of a 256×256 grid. In the inset the time series of n_{\max}/N is shown. The circled point is the "singular" event which is contained in the subset from which the dashed curve of Fig. 3 was extracted.

In summary we have obtained the two dimensional distribution of the local stretching rate in a $2D$ surface flow with compressibility $\mathcal{C} = 0.21$. The spectrum of the scaling exponents of the intermittent distribution of the coarse grained mass at small scales has been numerically computed. Our results indicate that the mass moments saturate at order $n_c \simeq 0.86$ in qualitative agreement with the prediction based on a Gaussian, white in time model of compressible flow.

Direct measurement of the coarse grained mass density at small scales confirms the results within the error bars up to order $n \simeq 1.3$. The events of high mass concentration at small scales have been identified by calculating the probability density of the maximum number of particles on grid resolution. The multi-fractal spectrum obtained from the coarse grained moments for those specific events is compatible with the existence of a saturation exponent as predicted by the stretching rate analysis.

* * *

This work was supported by the Deutsche Forschungsgemeinschaft. Numerical simulations have been performed at CINECA (INFM parallel computing initiative).

REFERENCES

- [1] BALKOVSKY A., FALKOVICH G. and FOUXON A., *Phys. Rev. Lett.*, **86** (2001) 2790
- [2] FALKOVICH G., GAWĘDZKI K. and VERGASSOLA M., *Rev. Mod. Phys.*, **73** (2001) 913.
- [3] OTT E., *Chaos in Dynamical Systems* (Cambridge University Press) 1993.
- [4] BEC J., *Phys. Fluids*, **15** (2003) L81.
- [5] KLYATSKIN V. I. and SAICHEV A. I., *JETP*, **84** (1997) 716
- [6] ELPERIN T., KLEEROIN N., L'VOV V.S., ROGACHEVSKII I. and SOKOLOFF D., *Phys. Rev. E*, **66** (2002) 036302
- [7] GOLDBURG W. I., CRESSMAN J. R., VÖRÖS Z., ECKHARDT B. and SCHUMACHER J., *Phys. Rev. E*, **63** (2001) 065303.
- [8] CRESSMAN J. R., DAVOUDI J., GOLDBURG W. I., and SCHUMACHER J., *New J. Phys.*, **6** (2004) 53
- [9] BOFFETTA G., DAVOUDI J., ECKHARDT B. and SCHUMACHER J., *Phys. Rev. Lett.*, **93** (2004) 134501
- [10] HENTSCHEL H.G.E. and PROCACCIA I., *Physica D*, **8** (1983) 435
- [11] BEC J., GAWĘDZKI K. and HORVAI P., *Phys. Rev. Lett*, **92** (2004) 224501.
- [12] BALKOVSKY E. and FOUXON A., *Phys. Rev. E*, **60** (1999) 4164.
- [13] K. Gawędzki, *Private communication*.
- [14] KRAICHNAN R.H., *Phys. Rev. Lett.*, **72** (1994) 1016.